PATTERN FORMATION IN NETWORKS OF CHAOTIC SPIKING-BURSTING NEURONS

M. I. RABINOVICH[1], J. J. TORRES[1], P. VARONA[1,2]
[1] *Institute for Nonlinear Science, UCSD. La Jolla, CA 92093-0402*
[2] *GNB. Dpto. de Ingeniería Informática, UAM, 28049 Madrid, SPAIN*
E-mail: jtorres@heisenberg.ucsd.edu

Chaotic neuron models can display a wide variety of coherent spatio-temporal patterns in networks with large number of units. We present a study of pattern formation and regularization phenomena using chaotic Hindmarsh-Rose model neurons. While the parameters of each neuron were initially set in the range of values where individual chaotic spiking-bursting activity was observed, the colective activity inside the networks produced coherent and well defined spatio-temporal patterns with the activity of each unit regularized. We investigated several types of network architectures and connections and we report an explanation for the observed phenomena.

1 Introduction

A wide variety of spatio-temporal patterns has been observed in the neuronal activity of the nervous system[1,2,3]. Such coherent spatio-temporal distributions of neural signals are thought to precisely bind, encode, store and process large amounts of information. On the other hand, it has also been observed that the behavior of some isolated neurons may be highly irregular and even chaotic[4,5]. The Hindmarsh-Rose (HR) model[6] reproduces the fundamental characteristics of the spiking-bursting activity of excitable cells and in particular those observed in the neurons of central pattern generators[5]. The HR model can also account for the chaotic behavior observed in some isolated cells. We have previously studied pattern formation in networks of electrically coupled chaotic HR Neurons[7]. Here we present a more detailed study in which different patterns of regularized activity are reported and explained for a wide variety of architectures and types of connections.

2 Network model

We have built a network of non-identical HR neurons with parameters selected randomly in the regime of chaotic oscillations. The dynamics of this model can be described by the following system of equations:

$$\begin{aligned}
\frac{dx_{ij}(t)}{dt} &= y_{ij}(t) + 3x_{ij}^2(t) - x_{ij}^3(t) - z_{ij}(t) + e_{ij} - g_{ij}(\mathbf{X}, \mathbf{\Omega}), \\
\frac{dy_{ij}(t)}{dt} &= 1 - 5x_{ij}^2(t) - y_{ij}(t), \\
\frac{1}{\mu}\frac{dz_{ij}(t)}{dt} &= -z_{ij}(t) + S\left[x_{ij}(t) + 1.6\right]
\end{aligned} \tag{1}$$

where the function $g_{ij}(\mathbf{X}, \mathbf{\Omega})$ represents the synaptic currents arriving to unit (i, j), $\mathbf{X}$ is a real matrix such that $(\mathbf{X})_{ij} = x_{ij}(t)$ and $\mathbf{\Omega}$ stands for a set of parameters

which characterizes the particular synapse. The neuron parameters are chosen to place the single units (when $g_{ij}(\mathbf{X}, \mathbf{\Omega}) = 0$) in the chaotic regime ($e_{ij} = 3.281 \pm 0.05$, $r = 0.0021$ and $S = 4$).

The isolated dynamics of a single HR neuron with this selection of parameters produces the characteristic irregular spiking-bursting activity shown in figure 1. This dynamics is characterized by two different time scales. The subsystem (x_{ij}, y_{ij}) is responsible for the generation of fast spikes, and the slow subsystem (x_{ij}, z_{ij}) is responsible for the slow waves over which the spikes appear. The fast subsystem is placed nearby the homoclinic bifurcation and, under the influence of the slow subsystem, produces a chaotic bursting-spiking behavior[8].

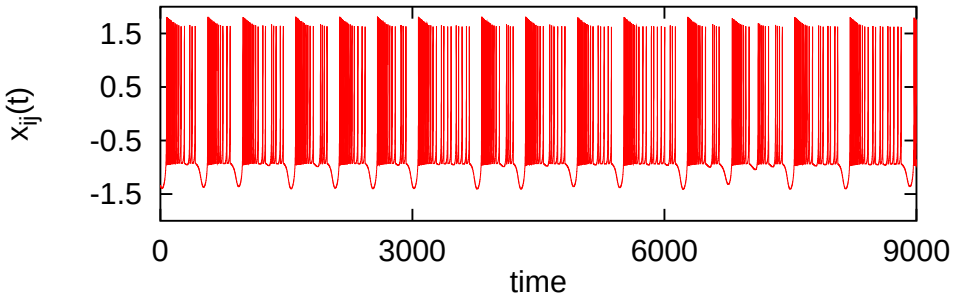

Figure 1. Time series of the chaotic activity (x_{ij}) of an isolated HR neuron.

For the network dynamics, the analytical form of $g_{ij}(\mathbf{X}, \mathbf{\Omega})$ depends on the kind of synapse considered, i.e., electrical or chemical. The electrical synapses are described by

$$g_{ij}(\mathbf{X}, \mathbf{\Omega}) = g_e \sum_{(lm)} [x_{ij}(t) - x_{lm}(t)], \quad \mathbf{\Omega} \equiv \{g_e\} \tag{2}$$

where g_e is the electrical coupling conductance. The sum in (2) extends over the neurons (lm) that are connected to neuron (ij). In the simulations described in this paper we considered two-dimensional lattices with periodic boundary conditions and nearest neighbor connections among the units. We built both square and hexagonal lattices with four and six nearest neighbors, respectively.

We will also characterize the activity of networks with chemical synapses among the neurons. In this case g_{ij} is described by the following expression:

$$g_{ij}(\mathbf{X}, \mathbf{\Omega}) = g_c \sum_{(lm)} s_{lm}(t) [x_{ij}(t) - x_{syn}], \tag{3}$$

where g_c is the maximal postsynaptic conductance and x_{syn} is the reversal potential of the synapses. The synaptic activation, $s_{lm}(t)$, is a sigmoidal function of the presynaptic potential x_{lm} and follows a first-order kinetics, i.e.,

$$\frac{ds_{lm}(t)}{dt} = \frac{\bar{s}_{lm}(t) - s_{lm}(t))}{\tau\,[1 - \bar{s}_{lm}(t)]}. \tag{4}$$

Here τ is the time constant characterizing the chemical synapse and $\bar{s}_{lm}(t) = 1/(1+\exp[\alpha\{x_0 - x_{lm}(t)\}])$. The parameters α and x_0 are adjusted to reproduce the shape of a real postsynaptic potential. Therefore, we have $\mathbf{\Omega} = \{g_c, x_{syn}, \tau, \alpha, x_0\}$ as the set of parameters characterizing each individual synapse.

In the next sections we analyze in detail the behavior of networks of such HR units connected either with electrical or chemical synapses.

3 Networks of electrically coupled neurons

We have previously reported the emergence of coherent spatio-temporal patterns in networks of electrically coupled HR units with $g_e > 0$ [7]. Figure 2 shows a typical snapshot of these patterns in a network of 100x100 units for $g_e = 1.5$. These patterns are formed by clusters of synchronization and regularization in the individual slow dynamics. The slow oscillations become regular (as seen in the bottom panel of figure 2) and then the spatio-temporal patterns emerge.

We have also investigated the same network architectures with negative electrical coupling $g_e < 0$. In this case, similar patterns have been found in a checkerboard configuration showing well defined spiral waves. These structures are only observed in networks with size larger than 30x30 units. The topology of the patterns on the background of the checkerboard is similar to the case in which $g_e > 0$. The checkerboard configuration emerges by a regularization mechanism in the slow dynamics induced from the antiphase oscillations among the nearest neighbors. These kind of patterns have also been observed in two-dimensional coupled maps[9].

Figure 3 shows the generation of traveling spiral waves using this kind of architecture ($g_e < 0$) for the connections. The network evolves from a disordered initial state to the spiral patterns depicted in the figure. The patterns emerge and separate the different checkerboard regions of the background made of out-of-phase oscillating neighbor units. The width of the wave depends on the strength of the coupling. When g_e is increased (in absolute value) the interphase becomes narrower. The waves link units that have the same oscillating behavior. Different kind of patterns can be observed (spirals, strips, collapsing squares, etc.) depending on the initial conditions and on the heterogeneity of the network. The bottom panels in figure 3 show the regular slow waves in the activity of member units.

4 Networks of neurons coupled with chemical synapses

When the neurons are coupled with chemical synapses (described by the equation 3) spiral patterns similar to those observed for the positive electrical connections are observed. We only considered excitatory chemical synapses ($x_{syn} = 0$) for this study. Spatio-temporal patterns corresponding to two different choices of the synaptic parameters (Ω) are shown in figure 4. Again, the slow single neuron oscillations become regular (see bottom panels in figure 4). Note that the spiking behavior

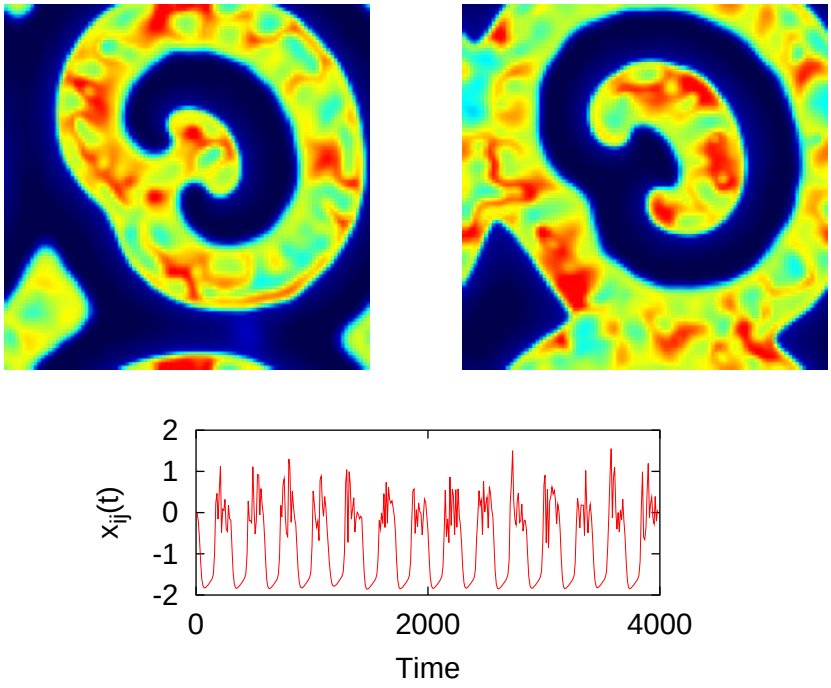

Figure 2. Top: temporal evolution of a periodic spatio-temporal pattern observed in a square network of 100x100 chaotic Hindmarsh-Rose units using the parameters specified in the text and $g_e = 1.5$. Bottom: activity of a single neuron inside this network where the regularization of the slow waves can be observed.

for these two examples is not the same. In spite of the different parameters used for the synapses and the corresponding different spiking behaviors, the patterns have similar structures since the slow oscillations are regular and have the same characteristic frequencies.

In these networks of neurons coupled with chemical synapses, the effect of mutual influence among units is not as fast as in the case of electrical coupling. This implies that the region of the state space in which spike (fast oscillation) synchronization can be observed is very small. However it is possible to find wide regions in which bursting (slow wave) synchronization is present.

5 Origin of the regularization

Although the origin of the regularization for the negative coupling can be intuitively understood from the competition emerging between the antiphase activities of the neighbors, the explanation for the regularization mechanisms in the case of positive coupling (electrical or chemical) is more subtle.

In order to understand the origin of these large-scale coherent structures in

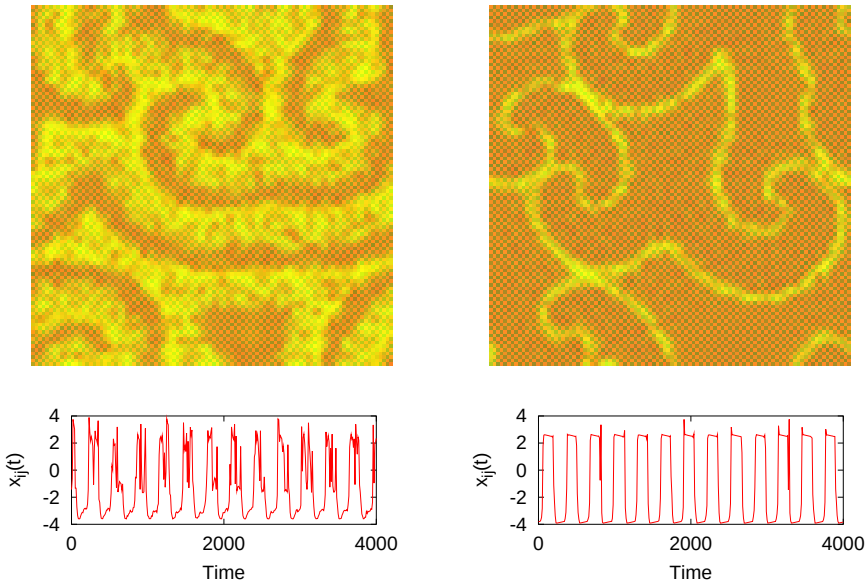

Figure 3. Checkerboard patterns in a network of 100×100 chaotic HR units with negative electrical couplings between nearest neighbor units. Left, network with $g_e = -0.95$. Right, network with a stronger absolute value for the coupling, $g_e = -1.12$. Bottom panels show the regular slow oscillations of single neuron activity in members of each network.

networks of electrically coupled neurons with positive g_e we investigated the cooperative behavior of a small cluster of such chaotic elements. We found that the regularization of the average activity occurs when the size of this cluster is sufficiently large. In contrast, small groups of neurons clearly exhibit three different kinds of chaotic dynamics depending on the value of the diffusive coupling g_e: (i) developed chaos whose dimension increases with the number of chaotic elements for a small value of the coupling, (ii) chaotic synchronization of the slow oscillation (bursts) for moderate coupling, and (iii) complete chaotic synchronization (both spikes and bursts) for strong coupling[10,11].

We call this cluster with average periodic (in time) behavior a *coarse grain* (CG). We suppose that the regular spatio-temporal patterns observed in our computer simulations are strongly related to the emergence of many interacting coarse grains inside the lattice for a moderate value of the coupling. The cooperative behavior of the diffusively coupled coarse grains (periodic generators in our case) produce the regular spatio-temporal patterns observed[12]. In order to show this, we can describe the coarse grain dynamics using the variables

$$X(t) = \frac{1}{M}\sum_{i=1}^{M} x_i(t) = \langle x_i \rangle_{CG}, \qquad Y(t) = \langle y_i \rangle_{CG}, \qquad Z(t) = \langle z_i \rangle_{CG},$$

where M is the number of elements in the cluster, and x_i represents the i-th HR neuron in this cluster. An approximate equation for the dynamics of X, Y, Z can

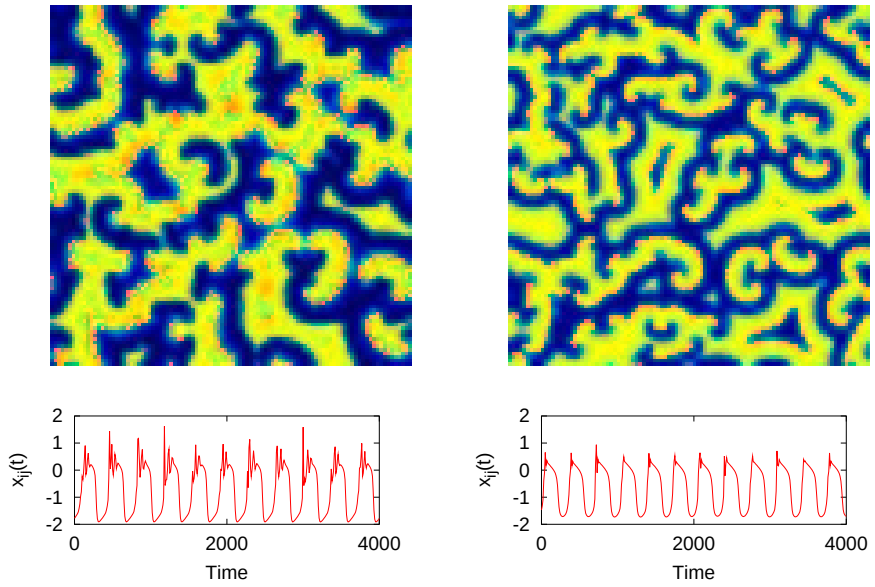

Figure 4. Spatio-temporal patterns in a 100x100 HR network with chemical synapses between nearest neighbor units for two different choices of the set $\mathbf{\Omega}$ and the same initial conditions: (Top) Snapshots showing the activity of the network. The parameters were chosen as follows: $\mathbf{\Omega}_1 = \{1.5, 0, 5, 1.5, 1.8\}$ (left), and $\mathbf{\Omega}_2 = \{1.6, 0, 20, 1., 1.75\}$ (right). (Bottom) Time series showing the regular activity of member neurons for the two cases.

be obtained by substituting

$$x_i = X(t)+\xi_i(t; g_e, M), \qquad y_i(t) = Y(t)+\eta_i(t; g_e, M), \qquad z_i(t) = Z(t)+\zeta_i(t; g_e, M),$$

in equations (2)-(2) which yields (ignoring higher order terms than ξ_i^2):

$$\frac{dX}{dt} = Y + 3X^2 + 3r(t; g_e, M) - X^3 - 3Xr(t; g_e, M) - Z + \epsilon \tag{5}$$

$$\frac{dY}{dt} = -5X^2 - Y - [5\, r(t; g_e, M) - 1], \tag{6}$$

$$\frac{1}{\mu}\frac{dZ}{dt} = -Z + S(X + 1.6), \tag{7}$$

where $\epsilon = \langle e_i \rangle_{CG}$. We have taken into account from the definition of X, Y, and Z that $\langle \xi_i(t) \rangle_{CG} = \langle \eta_i(t) \rangle_{CG} = \langle \zeta_i(t) \rangle_{CG} = 0$, and consequently the only function left to be determined is $r(t; g_e, M) = \langle \xi_i^2 \rangle_{CG}$.

In order to the describe the slow dynamics we need to make a reasonable assumption about the nonautonomous term on the right hand side of equation (5). Since $r(t; g_e, M)$ varies much more rapidly with time than the slow coarse grain oscillation, we suppose that the dynamics of a coarse grain depend on the time-averaged value of $r(t; g_e, M)$ defined as $R(t; g_e, M) = (1/t)\int_0^t r(t')dt'$ with $t_r << t < T$, where t_r is the characteristic time scale of the fast pulsation $r(t; g_e, M)$ (spiking behavior) and T is the characteristic time scale of X. In the system (5)-(7) we now

replace $r(t; g_e, M)$ by the slow function of time $R(t; g_e, M)$ which also depends on the strength of the diffusive coupling between elements and the size of the coarse grain. If our hypothesis is correct, $R \approx constant \neq 0$ for small values of g and $R \approx 0$ for large values of the coupling; for moderate values of the coupling prediction of the behavior of R is not intuitively clear. Our computer simulations indicate that for particular moderate values of g_e the behavior of R becomes periodic. This g_e-dependent behavior of R infers that the averaged dynamics X also will change as the coupling parameter is varied.

We can investigate the appearance of the periodic average behavior using equations (5)-(7) with $r(t; g_e, M)$ replaced by $R(t; g_e, M)$, the latter being a constant or a periodic function depending on the magnitude of the coupling being considered. For sufficiently small g_e, R is nearly constant taking on values in the range 0.4-0.5 and only a single stable fixed point appears, one corresponding to steady-state behavior of the cluster. For $R < R_{crit}$ ($g_e > g_{e,crit}$) this fixed point becomes unstable and the limit cycle in the 3D phase space of the average coarse grain system undergoes a supercritical and sharp Andronof-Hopf bifurcation to a stable fixed point. Strictly speaking, at the moment of this bifurcation, R becomes a periodic function of time. Nevertheless, close to the bifurcation point the influence of this periodicity on the existence of the limit cycle is not important. The direct calculations[12] confirmed this supposition.

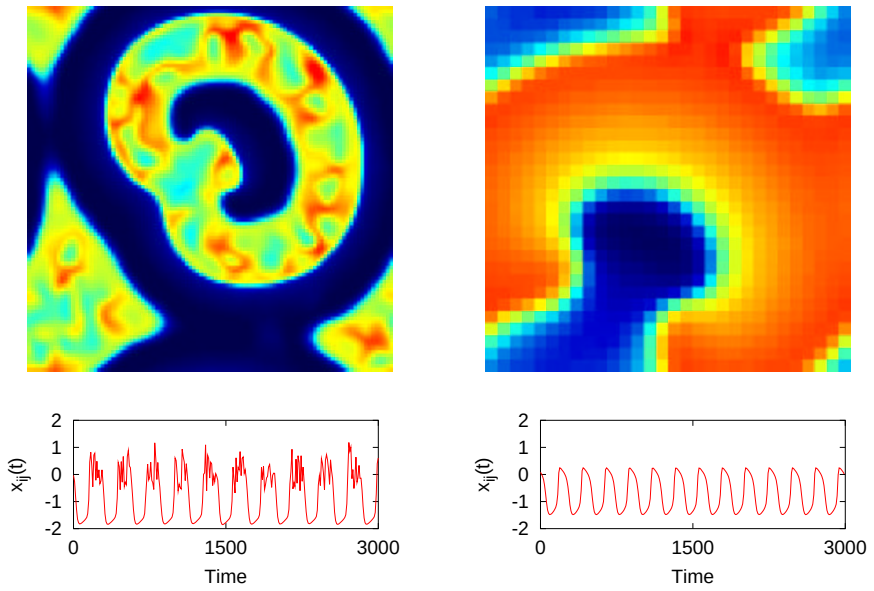

Figure 5. Left: periodic spatio-temporal pattern observed in a square network of 100x100 Hindmarsh-Rose elements with $g_e = 1.5$. Right: periodic spatio-temporal patterns observed in a square network of 30x30 coarse grain elements computed for $R = 0.23$ and $G = 0.5$ (the rest of the parameters have the same values used in the HR lattice).

The dynamical mechanism of the ordering averaged behavior of the coarse grain relies on the synchronization and regularization of the activity of the M units inside the grain. The degree of synchronization of a single neuron with the average activity of the whole grain depends on the strength of the coupling. In the case of regular behavior ($g_e \approx 0.1$) the single neuron activity is highly synchronized with the periodic mean field. For $g_e \approx 0.05$, the synchronization between mean field and individual behavior is absent and one observes spatio-temporal disorder. Thus, for a moderate value of g_e ($g_e \approx 0.1$ using the model parameters described above) the coarse grain behaves as a single element with periodic slow dynamics.

The existence of such structures of large regular spatio-temporal patterns in the diffusive networks is impossible in weakly coupled architectures because the local oscillations of neighboring elements are not correlated for small couplings g_e and the mean field of the coarse grains becomes homogeneous and stable. The level of spatially homogeneous chaos increased as $g_e \to g_0 \ll 1$.

For moderate values of the coupling the coarse grain assembly should exhibit regular spatio-temporal patterns. As confirmation of this conjecture, we have checked the behavior of a network consisting of coarse grain units with slow periodic behavior. The description of this network is analogous to that given by the network of HR units wherein (x_i, y_i, z_i) are replaced by (X_i, Y_i, Z_i). We are looking for patterns in the coarse grain network that have the same space scale (relative to the size of the lattice) as the pattern in the original HR lattice. Thus, the pattern in the coarse grain lattice should have identical structure but with a smaller absolute size. Since both patterns (on the original HR lattice and the coarse grain lattice) have the same time scale, we can say that the speed of front propagation in the HR lattice must be larger than for the coarse grain lattice. The propagation speed of the front increases together with the value of the diffusion. We can conclude, based on this scaling argument, that a coarse grain pattern with the same relative size as the original may be found only in the case when the coarse grain lattice coupling G is smaller than the diffusive coupling g in the original HR network. Figure 5 (right) shows a snapshot of the spatio-temporal pattern obtained for the square network of coarse-grain units reproducing the same topology that existed in the original HR network (see figure 5, left and figure 2). This pattern (obtained for $G = 0.5$) has the same topology and is clearly reminiscent of those produced by the original heterogeneous lattice of chaotic HR elements (for $g_e = 1.5$) displayed in the top row of figure 2 and in the left panel of figure 5.

6 Discussion

Neural activity displays a huge variety of spatio temporal patterns. Particularly, spiral patterns similar to those described above have been discovered in the cortex of animals and humans[1,3]. In this paper we have shown that coherent spatio-temporal patterns can arise in network architectures of chaotic HR units, in spite of their heterogeneity, the highly irregular individual behavior, or the particular type of connection. Periodic boundary conditions were applied to both H-R and coarse grain networks in all the simulations described in this paper. The topology of the patterns was not affected when we used fixed boundary conditions. We have

also observed the same behavior in hexagonal lattices (both coarse grains and H-R networks). In this case, the strength of the coupling has to be reduced to take into account the larger number (six) of nearest neighbors.

These coherent spatio-temporal structures arise as a result of regularization mechanisms on the slow dynamics by the cooperative activity of clusters of units inside the network. An electrical coupling with negative conductance induces regularization driven by the competition of the antiphase activities among neighbors. For positive coupling, the origin of this behavior can be explained introducing the concept of coarse grain dynamics, in which the averaged activity of the fast pulsations inside a cluster of neurons induces the regularization.

Acknowledgments

We are most appreciative to R. Huerta, and H. D. I Abarbanel for many discussions on the models. Mikhail Rabinovich acknowledges support from U.S. Department of Energy grant DE-FG03-96ER14592. J.J. Torres and P. Varona acknowledge support from Universidad de Granada and MEC, respectively. All authors received partial support from the CIA/Office of Research and Development through project No. 98-F135000-000.

References

1. J. C. Prechtl, L. B. Cohen, B. Pesaran, P. P. Mitra and D. Kleinfeld, *Proc. Natl. Acad. Sci. USA*, **94**, 7621 (1997).
2. E. Vaadia, I. Haalman, M. Abeles, H. Bergman, Y. Prout, H. Slovin, A. Aertsen. *Nature* **373**, 515 (1995).
3. I. A. Shevelev, E. N. Tsicalov, A. M. Gorbach, K. P. Budko and G. A. Sharaev. *J. Neurosci. Methods.* **46**, 49 (1992).
4. R. Elson, A.I. Selverston, R. Huerta, M.I. Rabinovich, H.D.I. Abarbanel. *Physical Review Letters* **81**: 5692 (1998).
5. H.D.I. Abarbanel, R. Huerta, M.I. Rabinovich, N.F. Rulkov, P. Rowat, and A.I. Selverston. 1996. *Neural Computation* **8**:1567-1602.
6. J.L. Hindmarsh and R.M. Rose *Proc.R.Soc.Lond.* **B221**, 87 (1984).
7. R. Huerta, M. Bazhenov and M.I. Rabinovich, *Europhys.Lett.* **23**(1), 1 (1998).
8. M. Bazhenov, R. Huerta, M.I. Rabinovich and T. Sejnowski *Physica* **D116**, 392 (1998).
9. V.I. Sbitnev *Int.J.Bifurcation and Chaos*, **7**(11), 2569 (1997).
10. V. S. Afraimovich, N. N. Verichev and M.I. Rabinovich. Inv. VUZ Radiofiz. RPQAEC **29**, 795 (1986).
11. L. M. Pecora and T. L. Carroll. Phys. Rev. Lett. **64**, 821 (1990).
12. M.I. Rabinovich, J.J. Torres, P. Varona, R. Huerta, P. Weidman. Submitted to Phys. Rev E.